

Ex vivo T2*-w MRI and Quantitative Susceptibility Mapping reflect histological iron accumulation in Frontotemporal Dementia

Primary: Neuro - Dementia **Secondary:** Contrast Mechanisms - Susceptibility/QSM **Digital Poster** · 60 min | Detectable Changes in Dementia · Wednesday, May 13 at 08:20 AM **Keywords:** NEURODEGENERATION FRONTOTEMPORAL DEMENTIA QUANTITATIVE SUSCEPTIBILITY MAPPING (QSM) EX VIVO MRI T2-STAR

Fieke Prinse  ^{1,2}, **Lucia Giannini**¹, **Marjolein Bulk**¹, **Ernst Suideest**^{2,3}, **Kyra Dijkstra**⁴, **Renee van Buuren**¹, **Niels Dekker**⁵, **Marius Staring**⁵, **Chloe Najac**², **John van Swieten**¹, **Elise Doppler**¹, **Harro Seelaar**¹, **Louise van der Weerd**^{2,6}

¹Department of Neurology, Erasmus University Medical Center, Netherlands

²C.J. Gorter MRI Center, Department of Radiology, Leiden University Medical Center, Leiden, Netherlands

³Central Animal Facility, Leiden University Medical Center, Leiden, Netherlands

⁴Department of Pathology, Leiden University Medical Center, Leiden, Netherlands

⁵Division of Image Processing, Department of Radiology, Leiden University Medical Center, Leiden, Netherlands

⁶Department of Human Genetics, Leiden University Medical Center, Leiden, Netherlands

 **Presenting Author:** Fieke Prinse (f.prinse@erasmusmc.nl)

Impact

This study shows increased iron accumulation in FTLD vs controls. Ex vivo T2*-w MRI and QSM have complementary value to visualize the histological changes. Our next step will be to investigate iron accumulation *in vivo* in FTLD using 7T MRI.

Synopsis

Motivation: Histological analysis of ex vivo tissue is the standard approach for investigating iron deposition in frontotemporal lobar degeneration (FTLD), yet *in vivo* evaluation is vital for elucidating disease-related processes.

Goals: This study aimed to compare ex vivo T2*-w MRI and quantitative susceptibility mapping (QSM) to histology of FTLD cases and controls.

Approach: We analyzed line profiles of gray intensity values drawn over the cortical depth on registered T2*-w MRI, QSM, and histological iron staining data for patients and controls.

Results: We found increased iron accumulation in FTLD compared to controls, which can be visualized with ex vivo 7T MRI.

Background

Frontotemporal lobar degeneration (FTLD) is the second most common cause of early onset dementia, characterized by frontotemporal atrophy and accumulation of aggregated proteins TDP-43 (FTLD-TDP) or tau (FTLD-tau)¹. Besides these protein aggregates, several small histological or MRI studies showed accumulation of iron in the brain based on qualitative visual assessment of cortical patterns²⁻⁴. In this study, we used histology, T2*-w MRI, and quantitative susceptibility mapping (QSM) to evaluate iron accumulation patterns in a quantitative manner.

Methods

Postmortem data: Tissue blocks obtained via the Netherlands Brain Bank from the frontal and temporal cortex of 14 FTLD cases (6 FTLD-tau; 8 FTLD-TDP) and 11 healthy controls (HC) were included ([figure 1](#)).

MRI: We used a 7T PharmaScan Bruker MRI system with ParaVision (Bruker BioSpin, Ettlingen, Germany), equipped with a 38 mm transmit-receive volume coil. MGE scans (scan time: 10h) were acquired (FTLD: TE₁: ΔTE:TE_{max}=3.5:5:43.5ms, TR =150ms, resolution: 100μm³, 9 echoes; HC: TE₁: ΔTE:TE_{max} = 12.5:10.7:44.6ms, TR=75.0ms, 100μm³ resolution, 4 echoes). QSM maps were reconstructed using the SEPIA toolbox: FSL BET⁵, Optimum weights Laplacian (MEDI)⁶, VSHARP⁷, and MEDI⁸⁻¹⁰.

Histology: After MRI, all tissue blocks were cut into 20μm sections. Cortical iron accumulation was detected using an in-house developed DAB enhanced Prussian Blue histology protocol¹¹.

Registration and line profiles: Slices of the seventh (FTLD) or third echo (HC) of the 3D T2*-w and QSM most similar to the histology (downsampled to match MRI resolution) were selected. Histological slides were converted to grayscale. QSM slices are depicted between [-0.065, 0.065]. Images were registered using rigid and affine registration with ITK-elastix^{12,13}. Based on three selected reference points (GM/air surface, GM/WM border and half the WM depth) a 40-point line with a width of five pixels was drawn using FIJI¹⁴. Gray intensity values (GIV) were obtained per point (averaged over the line width) for each modality. The obtained GIV per modality were scaled between 0 and 1, based on the highest and lowest value. Lower GIV (i.e. dark appearance) on the histological and T2*-w image reflected more iron. Higher GIV (light appearance) on the QSM reflected iron, while lower GIV (dark on image) reflected myelin.

Statistical Analysis: We compared the line profiles of FTLD versus HC by calculating the area between curves (ABC). To compare this area, we randomly reassigned the labels (FTLD, HC) and permuted this test 10,000 times to generate a normal distribution. Then we tested our real area to the obtained normal distribution using a student's t-test. To compare the correspondence between the three modalities, we calculated the Pearson's correlation per case and averaged these correlations per modality. The level of significance was set at p < 0.05.

Results

FTLD vs HC: Examples of the modalities and line profiles of a HC and FTLD case are shown in [figure 2](#) and [figure 3](#). In HC, cortical layers are clearly distinguishable with GIV drops around point 10 and 20 reflecting lines of Ballinger. The GM/WM border is visible as a steep drop in GIV at point 30. Average line profiles showed significantly lower GIV in FTLD compared to HC in the temporal lobe on histology (p<0.001) and T2*-w MRI (p=0.032), whereas there was no difference in the frontal lobe. Line profiles of QSM showed lower GIV in FTLD versus HC (p=0.013) in the frontal lobe, but no difference for the temporal lobe. At the GM/WM border, the FTLD group showed an increase in GIV, corresponding with the location of U-fibers ([figure 4](#)).

Across modalities: There was a good mean correlation between histology and T2*-w MRI frontal: $r=0.91$, $R^2=0.83$, $p<0.001$; temporal: $r=0.88$, $R^2=0.8$, $p<0.001$). There was a weak correlation between histology and QSM for both frontal ($r=0.39$, $R^2=0.23$, $p<0.001$) and temporal ($r=0.43$, $R^2=0.24$, $p<0.001$) and for T2*-w MRI and QSM for both frontal ($r=0.38$, $R^2=0.22$, $p<0.001$) and temporal ($r=0.43$, $R^2=0.25$, $p<0.001$).

Discussion and Conclusion

This study showed increased iron accumulation in FTLD compared to HC visualized by line profiles on ex vivo T2*-w MRI, QSM, and histology. This result is in line with studies using visual scoring systems⁴, but with the advantage that the applied method is more robust therefore decreasing scoring bias. Furthermore, we demonstrated that histological iron accumulation can be visualized using 7T T2*-w MRI and QSM. T2*-w has a good overall correlation with histology, but certain specific details, such as U-fibers, can be better observed with QSM. Our next step will be to explore these iron accumulation patterns and line profiles in a large in vivo FTLD cohort.

Acknowledgements

Funding for this study was provided by Alzheimer Nederland from grant: WE.03-2020-10 and ZonMw from grant: 733050513.

References

1. Grossman M, Seeley WW, Boxer AL, Hillis AE, Knopman DS, Ljubenov PA, Miller B, Piguet O, Rademakers R, Whitwell JL, Zetterberg H, van Swieten JC. Frontotemporal lobar degeneration. *Nat Rev Dis Primers*. 2023 Aug 10;9(1):40. doi: 10.1038/s41572-023-00447-0. PMID: 37563165. [\[pmid\]](#)
2. Tisdall MD, Ohm DT, Lobrovich R, Das SR, Mizsei G, Prabhakaran K, Ittyerah R, Lim S, McMillan CT, Wolk DA, Gee J, Trojanowski JQ, Lee EB, Detre JA, Yushkevich P, Grossman M, Irwin DJ. Ex vivo MRI and histopathology detect novel iron-rich cortical inflammation in frontotemporal lobar degeneration with tau versus TDP-43 pathology. *Neuroimage Clin*. 2022;33:102913. doi: 10.1016/j.nicl.2021.102913. Epub 2021 Dec 14. PMID: 34952351; PMCID: PMC8715243. [\[pmid\]](#)
3. Giannini LAA, Bulk M, Kenkhuis B, Rajcic A, Melhem S, Hegeman-Klein I, Bossoni L, Suideest E, Dopper EGP, van Swieten JC, van der Weerd L, Seelaar H. Cortical iron accumulation in MAPT- and C9orf72-associated frontotemporal lobar degeneration. *Brain Pathol*. 2023 Jul;33(4):e13158. doi: 10.1111/bpa.13158. Epub 2023 Mar 27. PMID: 36974379; PMCID: PMC10307524. [\[pmid\]](#)
4. Prinse, F.A.M., Giannini, L.A.A., Bulk, M., et al. (2024, May 4 - 9) Analysis of Iron Accumulation in MAPT- and C9orf72-associated frontotemporal lobar degeneration: QSM, T2*-w MRI, and histology [Digital Poster Presentation]. ISMRM 2024, Singapore, Singapore. DOI: <https://doi.org/10.58530/2024/2616>
5. Smith SM. Fast robust automated brain extraction. *Hum Brain Mapp*. 2002 Nov;17(3):143-55. doi: 10.1002/hbm.10062. PMID: 12391568; PMCID: PMC6871816. [\[pmid\]](#)
6. Schofield MA, Zhu Y. Fast phase unwrapping algorithm for interferometric applications. *Opt Lett*. 2003 Jul 15;28(14):1194-6. doi: 10.1364/ol.28.001194. PMID: 12885018. [\[pmid\]](#)
7. Li W, Wu B, Liu C. Quantitative susceptibility mapping of human brain reflects spatial variation in tissue composition. *Neuroimage*. 2011 Apr 15;55(4):1645-56. doi: 10.1016/j.neuroimage.2010.11.088. Epub 2011 Jan 9. PMID: 21224002; PMCID: PMC3062654. [\[pmid\]](#)
8. Liu T, Liu J, de Rochefort L, Spincemaille P, Khalidov I, Ledoux JR, Wang Y. Morphology enabled dipole inversion (MEDI) from a single-angle acquisition: comparison with COSMOS in human brain imaging. *Magn Reson Med*. 2011 Sep;66(3):777-83. doi: 10.1002/mrm.22816. Epub 2011 Apr 4. PMID: 21465541. [\[pmid\]](#)
9. Liu J, Liu T, de Rochefort L, Ledoux J, Khalidov I, Chen W, Tsioris AJ, Wisniewski C, Spincemaille P, Prince MR, Wang Y. Morphology enabled dipole inversion for quantitative susceptibility mapping using structural consistency between the magnitude image and the susceptibility map. *Neuroimage*. 2012 Feb 1;59(3):2560-8. doi: 10.1016/j.neuroimage.2011.08.082. Epub 2011 Sep 8. PMID: 21925276; PMCID: PMC3254812. [\[pmid\]](#)
10. Liu Z, Spincemaille P, Yao Y, Zhang Y, Wang Y. MEDI+0: Morphology enabled dipole inversion with automatic uniform cerebrospinal fluid zero reference for quantitative susceptibility mapping. *Magn Reson Med*. 2018 May;79(5):2795-2803. doi: 10.1002/mrm.26946. Epub 2017 Oct 11. PMID: 29023982; PMCID: PMC5821583. [\[pmid\]](#)
11. van Duijn S, Nabuurs RJ, van Duinen SG, Natté R. Comparison of histological techniques to visualize iron in paraffin-embedded brain tissue of patients with Alzheimer's disease. *J Histochem Cytochem*. 2013 Nov;61(11):785-92. doi: 10.1369/0022155413501325. Epub 2013 Jul 25. PMID: 23887894; PMCID: PMC3808575. [\[pmid\]](#)
12. K. Ntatsis, N. Dekker, V. Valk, T. Birdsong, D. Zukić, S. Klein, M Staring, M McCormick. "itk-elastix: Medical image registration in Python", Proceedings of the 22nd Python in Science Conference, pp. 101 - 105, 2023, <https://doi.org/10.25080/gerudo-f2bc6f59-00d>.
13. Shamonin DP, Bron EE, Lelieveldt BP, Smits M, Klein S, Staring M; Alzheimer's Disease Neuroimaging Initiative. Fast parallel image registration on CPU and GPU for diagnostic classification of Alzheimer's disease. *Front Neuroinform*. 2014 Jan 16;7:50. doi: 10.3389/fninf.2013.00050. PMID: 24474917; PMCID: PMC3893567. [\[pmid\]](#)
14. Schindelin, J., Arganda-Carreras, I., Frise, E. et al. Fiji: an open-source platform for biological-image analysis. *Nat Methods* 9, 676–682 (2012). <https://doi.org/10.1038/nmeth.2019>

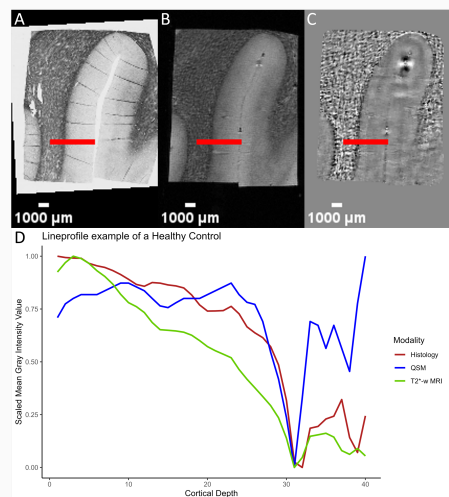
Figures and Tables

	FTLD-Tau	FTLD-TDP	Controls	P-value
N	6	8	11	
Female (%)	0 (0%)	4 (50%)	6 (55%)	0.3656
Male (%)	6 (100%)	4 (50%)	5 (45%)	0.3656
Age at death (years)	59.7 ± 11.8	70.5 ± 3.25	80.7 ± 9.3*	0.0007*
Postmortem delay (hh:mm)	5.53 ± 0.35	5.98 ± 0.99	6.66 ± 1.49	0.0995
Clinical diagnosis				
bvFTD (%)	5 (83%)	4 (50%)		
PPA (%)	0	4 (50%)		
PSP (%)	1 (17%)			
Sporadic	1	4		
Mutation	5	4		
MAPT	5			
C9orf72		2		
GRN		1		
TUBA4A		1		



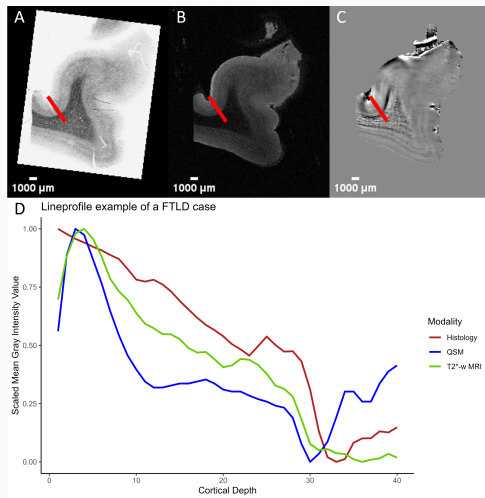
Scan for high-resolution version

Figure 1: Patient characteristics of the cohort. FTLD: frontotemporal lobar degeneration. Tau: tubulin associated unit. TDP: TAR DNA binding protein. BvFTD: behavioral variant frontotemporal dementia. PPA: primary progressive aphasia. PSP: progressive supranuclear palsy. MAPT: microtubule associated protein tau. C9orf72: chromosome 9 open reading frame 72. GRN: progranulin. TUBA4A: tubulin alpha 4a



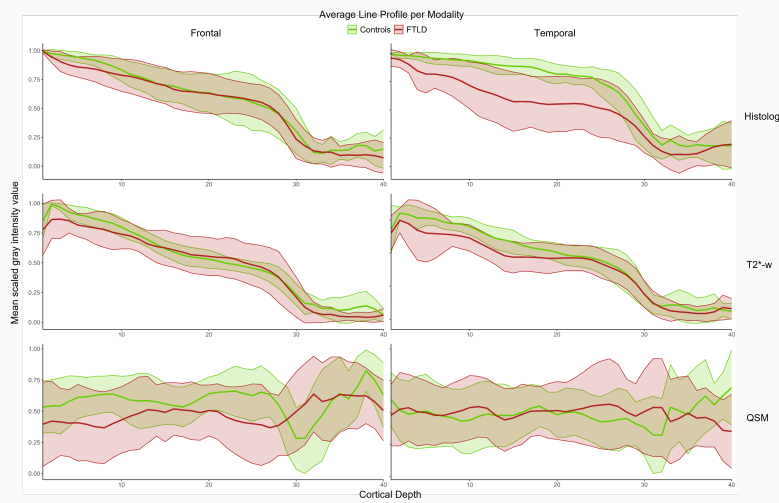
Scan for high-resolution version

Figure 2: Line profile examples of a control for histology (A), T2*-w magnitude (B), QSM (C). Red line depicts the selected region for the line profile. (D) Plot of the scaled mean gray intensity values over the cortical depth. Point 1 is the gray matter/air border. Point 10 and 20 reflect the lines of Ballinger. Point 30 reflects the gray/white matter border. Point 40 is at 1/2 of the depth of the white matter. QSM scale: [-0.065 0.065]. QSM: quantitative susceptibility mapping.



Scan for high-resolution version

Figure 3: Line profile examples of a FTLD case for histology (A), T2*-w magnitude (B), QSM (C). Red line depicts the selected region for the line profile. (D) Plot of the scaled mean gray intensity values over the cortical depth. Point 1 is the gray matter/air border. Point 30 reflects the gray/white matter border, clearly showing an increase for QSM, reflecting the U-fibers. Point 40 is at 1/2 of the depth of the white matter. QSM scale: [-0.065 0.065]. QSM: quantitative susceptibility mapping.



Scan for high-resolution version

Figure 4: Average mean scaled gray intensity value over the cortical depth per modality (rows) and region (columns) for the FTLD cases (red) and controls (green). The FTLD cases have lower mean gray intensity values for the temporal cortex on both the histology and the T2*-w MRI, reflecting iron accumulation. For the frontal QSM, there is a lower gray intensity value for the FTLD cases compared to HC, mostly due to the U-fibers found in the WM (point 30). Mean is plotted with the standard deviation.